

1

2

가
: 43 104 , 55
49 . 83
21
가 29 , 15 ,
4 , 가 3
(reactive hyperplasia) 21 , 7 , (Kikuchi's disease)
12 , 9

1.5 T Magnetom Vision(Siemens, Erlangen, Germany) MRI

TR 500 msec, TE 12 msec, flip angle 20 °

FLASH 2D

11.2 μT, 250 Hz

band-width, off-set 2.0 KHz

3

2

(CoMTR)

0.33(SD: ±0.04)

0.28(SD: ±0.05)

(P<0.05).

(P>0.05).

0.31

83%,

75%,

79%

, 0.31

가

가

가

가

(Magnetic resonance imaging, MRI)

가

가

가

. MRI

50%

가

T1

T2

가

가

(1).

, Damadian(2) MRI

가

1

2

T1, T2
(proton density weighted image)

(3,4).
(magnetization transfer image, MT image)
(5,6)
(magnetization transfer ratio, MTR)

가 (7,8).

, MRI

1996 7 1998 7

110

가

43

104

가

30

13

47 (5-80)

10

73

:

21 CT MRI
10 , 11

. 104

55

49

가 29 가

15

(reactive hyperplasia) 21

(Kikuchi 's disease) 12 ,

가 ,

9

7 ,

7

21 12

(Table 1)(Fig. 1).

가

1.5 T Magnetom Vision(Siemens, Erlangen, Germany) MRI

Table 1. Lymph Nodes Studied by Magnetization Transfer Imaging

Histopathology No. of Lymph Nodes	
Malignant Nodes	55
Lymphoma	15
Lymph nodes metastasis	40
Squamous cell carcinoma	29
Undifferentiated carcinoma	4
Melanoma	3
Leukemia	4
Benign Nodes	49
Tuberculosis	7
Reactive hyperplasia	21
Kikuchi 's disease	12
Acute lymphadenitis	9
Total	104

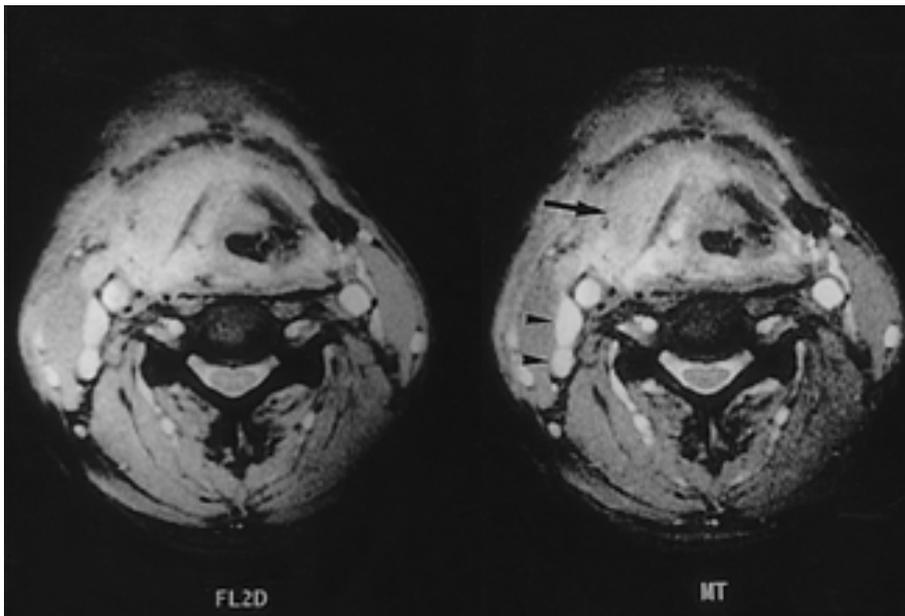


Fig. 1. Reactive hyperplasia. Enlarged right posterior cervical lymph nodes (arrowheads, CoMTR= 0.24) are seen in the patient with supraglottic squamous cell carcinoma penetrating thyroid cartilage (arrow).

T1 (FLASH 2D), T2

T1 가 가 2

T1, T2 가

TR 500 msec, TE 12 msec, flip angle 20° (corrected)

FLASH 2D MTR, CoMTR)

(preMT image) 11.2 μ T, 250 Hz CoMTR = 1 - { [Ms / SDs] / [Mo / SDo] }

band-width, off-set 2.0 KHz (magnetization transfer pulse) (postMT image) CoMTR :

5 mm, interslice gap 0.5 mm SDs :

(Average standard deviation of back ground noise with magnetization transfer)

CT T1, T2 SDo :

(Average standard deviation of back ground noise without magnetization transfer)

3

Wilcoxon rank sum test

(noise) 가 가 (Fig. 2). Kruskal-Wallis test

MTR = 1 - (Ms/Mo) (cut-off value) (Fig. 3).

MTR : (Magnetization transfer ratio)

Ms : (Signal intensity with magnetization transfer)

Mo : (Signal intensity without magnetization transfer)

55	10	45	0.31
----	----	----	------

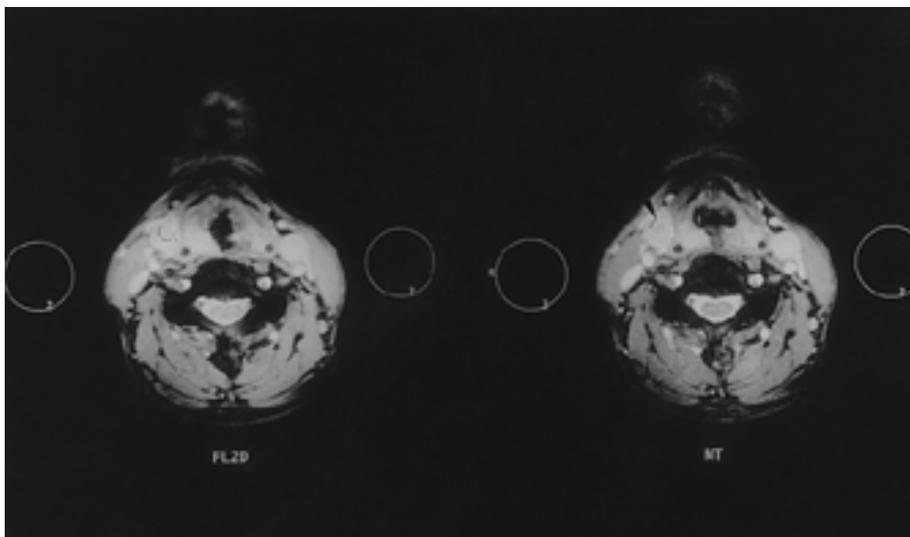


Fig. 2. Measurements of CoMTR. Supraglottic squamous cell carcinoma with both internal jugular lymph node metastases (CoMTR= 0.42). Notice the same size, shape, and location of ROI on both FLASH 2D and MT images (arrowhead).

0.23 0.49 . 0.30
 10
 가 2 , 7
 가 1 . 2
 49 12 37 0.30
 0.15 0.36 . 0.31
 12 4 ,
 3 , 3 , 2
 0.33(SD: ±
 0.04) 0.28(SD: ± 0.05) Wilcoxon
 rank sum test
 (P<0.05)(Table 2)(Fig. 1,2,4).
 Kruskal-Wallis test
 (P>0.05) 가
 (P>0.05)(Table 3).
 Kruskal-Wallis test
 (P>0.05)
 (P>0.05)(Table 4).
 (sternocleidomastoid muscle)
 0.46(SD: ± 0.04)
 0.04(SD: ± 0.02)
 (Table 2)(Fig. 5).

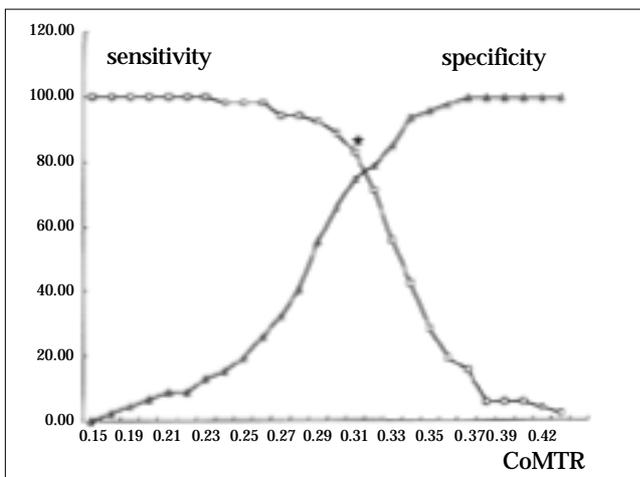


Fig. 3. Sensitivity and specificity curves of CoMTR for differentiation between malignant and benign lymph nodes. Cut-off value (star) for diagnosis of malignant nodes is 0.31.

0.31
 83%, 75% 79% (Fig. 3).

1/3 300

CT CT

CT

CT
 64-90%

Table 2. Mean MTR & CoMTR of Nodes, Muscle, and CSF

	MTR (SD)	CoMTR (SD)
Malignant nodes	0.35 (0.03)	0.33 (0.04)
Benign nodes	0.28 (0.06)	0.28 (0.05)
SCM muscle	0.46 (0.04)	
CSF	0.04 (0.02)	

SD : Standard deviation P < 0.05

MTR : Magnetization transfer ratio

CoMTR : Corrected MTR

P value : P value of CoMTR

Table 3. Mean CoMTR of Malignant Nodes

	CoMTR (SD)	W-R test	K-W test
Squamous cell carcinoma	0.34 (0.04)	P > 0.05	P > 0.05
Lymphoma	0.35 (0.05)		
Melanoma	0.38 (0.04)		
Leukemia	0.35 (0.02)		
Undifferentiated carcinoma	0.33 (0.02)		

W-R test : Wilcoxon rank sum test

K-W test : Kruskal-Wallis test

CoMTR : Corrected MTR

Table 4. Mean CoMTR of Benign Nodes

	CoMTR (SD)	W-R test	K-W test
Tuberculosis	0.29 (0.07)	P > 0.05	P > 0.05
Reactive hyperplasia	0.23 (0.06)		
Kikuchi 's disease	0.26 (0.02)		
Acute lymphadenitis	0.28 (0.02)		

19% MRI 가 , (9-17). (proton) (free water proton) (restricted water proton) MRI (macromolecular proton) (amplitude) T1, T2 (line width) (immobile macromolecular proton) CT 가 가 CT CT (17). (saturation) (RF pulse) (immobile proton) (myelin), , ,) (macromolecule, :

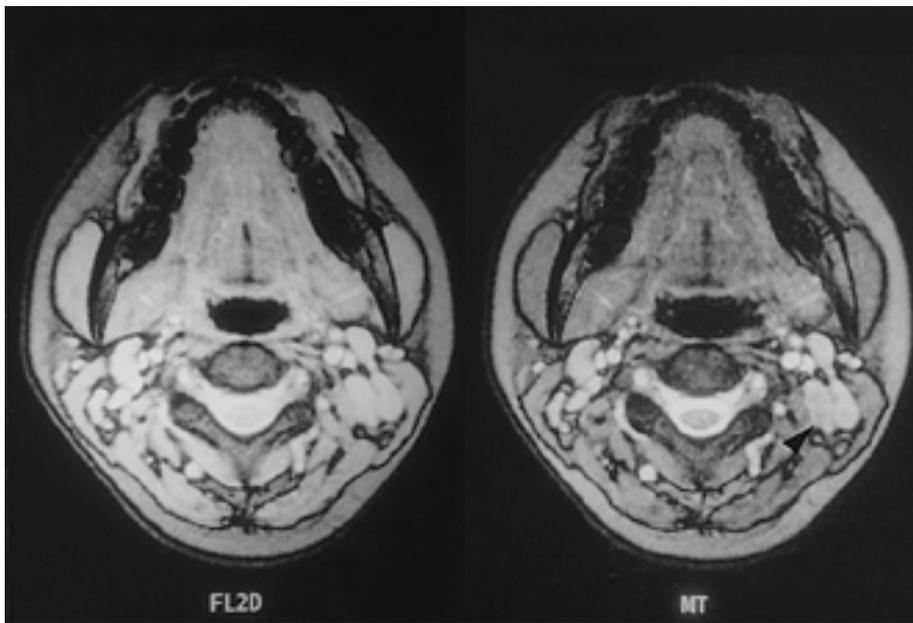


Fig. 4. Tuberculous lymphadenitis. The left posterior cervical lymph nodes (arrowhead) are enlarged and excisional biopsy reveals tuberculous lymphadenitis (CoMTR= 0.24).

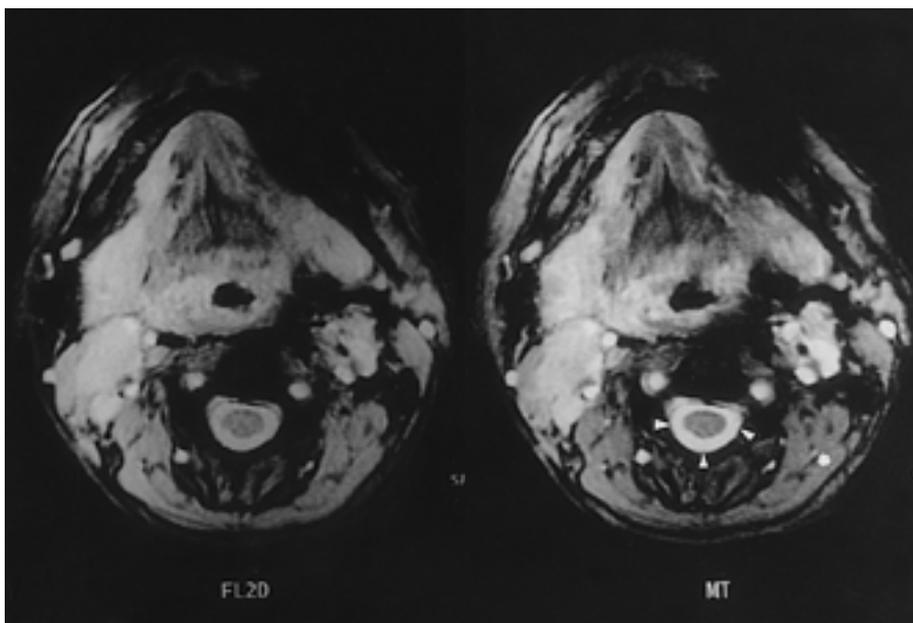


Fig. 5. FLASH 2D and MT images of muscle and CSF. Markedly suppressed signal intensity of the posterior neck muscles (asterisk) in contrast to bright signal intensity of CSF (arrowheads) on MT image, compared to FLASH 2D image.

가
가

(7,25).

(26,27)

가

0.31
0.30
0.31
83%, 75%, 79%

MRI

가

0.30

1. Som PM. *Lymph nodes*. In Som PM, Curtin HD. *Head and neck imaging*. St. Louis: Mosby, 1996:772-793
2. Damadian R. Tumor detection by nuclear magnetic resonance. *Science* 1971;171:1151-1153
3. Just M, Thelen M. Tissue characterization with T1, T2, and proton density values: results in 160 patients with brain tumors. *Radiology* 1988;169:779-785
4. Glazer GM, Orringer MB, Chenevert TL, et al. Mediastinal lymph nodes: relaxation time/pathologic correlation and implications in staging of lung cancer with MR imaging. *Radiology* 1988;168:429-431
5. Grossman RI, Gomori JM, Ramer KN, Lexa FJ, Schnall MD. Magnetization transfer: theory and clinical applications in neuroradiology. *RadioGraphics* 1994;14:279-290
6. Wolff SD, Balaban RS. Magnetization transfer imaging: practical aspects and clinical applications. *Radiology* 1994;192:593-599
7. Yousem DM, Montone KT, Sheppard LM, Rao VM, Weinstein GS, Hayden RE. Head and neck neoplasms: magnetization transfer analysis. *Radiology* 1994;192:703-707
8. Kobayashi S, Takeda K, Sakuma H, Kinosada Y, Nakagawa T. Uterine neoplasms: magnetization transfer analysis of MR images. *Radiology* 1997;203:377-382
9. Som PM. Lymph nodes of the neck. *Radiology* 1987;165:593-600
10. Van den Brekel MWM, Stel HV, Castelijns JA, et al. Cervical

- lymph node metastases: assessment of radiologic criteria. *Radiology* 1990;177:379-384
11. Mancuso AA, Harnsberger HR, Muraki AS, Stevens MH. Computed tomography of cervical and retropharyngeal lymph nodes: normal anatomy, variants of normal, and application in staging head and neck cancer. part II. Pathology. *Radiology* 1983;148:715-723
12. Reede DL, Bergeron RT. *Computed tomography of cervical lymph nodes*. In: *lymphatic imaging: lymphography, computed tomography, and scintigraphy*. 2nd ed. Baltimore: Williams & Wilkins, 1985:472-495
13. Friedman M, Shelton VK, Mafee M, Bellity P, Grybauskar V, Skolnik E. Metastatic neck disease: evaluation by computed tomography. *Arch Otolaryngol Head Neck Surg* 1984;110:443-447
14. Close LG, Merkel M, Vuitch MF, Reisch J, Schaefer SD. Computed tomographic evaluation of regional lymph node involvement in cancer of the oral cavity and oropharynx. *Head Neck* 1989;11:309-317
15. Stevens MH, Harnsberger R, Mancuso AA, Davis RK, Johnson LP, Parkin JL. Computed tomography of cervical lymph nodes: staging and management of head and neck cancer. *Arch Otolaryngol Head Neck Surg* 1985;111:735-739
16. Feinmesser R, Freeman JL, Nojek AM, Birt BD. Metastatic neck disease: a clinical/radiographic/pathologic correlative study. *Arch Otolaryngol Head Neck Surg* 1987;113:1307-1310
17. Som PM. Detection of metastasis in cervical lymph nodes: CT and MRI criteria and differential diagnosis. *AJR* 1992;158:961-969
18. Lundbom N. Determination of magnetization transfer contrast in tissue: an MR imaging study of brain tumors. *AJR* 1992;159:1279-1285
19. Lexa FJ, Grossman RI, Rosenquist AC. MR of Wallerian degeneration in the feline visual system: characterization by magnetization transfer rate with histopathologic correlation. *AJNR* 1994;15:201-212
20. Outwater E, Schnall MD, Braitman LE, Dinsmore BJ, Kressel HY. Magnetization transfer of hepatic lesions: evaluation of a novel contrast technique in the abdomen. *Radiology* 1992;182:535-540
21. Boorstein JM, Wong KT, Grossman RI, Bolinger L, McGowan JC. Metastatic lesions of the brain: imaging with magnetization transfer. *Radiology* 1994;191:799-803
22. Chan JKC, Tsang WYW. *Reactive lymphadenopathies*. In Weiss LM. *Pathology of lymph nodes*. New York: Churchill Livingstone, 1996: 81-168
23. Lee AS, Weissleder R, Brady TJ, Wittenberg J. Lymph nodes: microstructural anatomy at MR imaging. *Radiology* 1991;178:519-522
24. Mattila KT, Lukka R, Hurme T, Komu M, Alanen A, Kalimo H. Magnetic resonance imaging and magnetization transfer in experimental myonecrosis in the rat. *MRM* 1995;33:185-192
25. Yousem DM, Schnall MD, Dougherty L, Weinstein GS, Hayden RE. Magnetization transfer imaging of the head and neck: normative data. *AJNR* 1994;15:1117-1121
26. Yamashita Y, Fan ZM, Yamamoto H, et al. Spin-echo and dynamic gadolinium-enhanced FLASH MR imaging of hepatocellular carcinoma: correlation with histopathologic findings. *J Magn Reson Imaging* 1994;4:83-90
27. Stark DD, Wittenberg J, Edelman RR, et al. Detection of hepatic metastases: analysis of pulse sequence performance in MR imaging. *Radiology* 1986;159:365-370

Magnetization Transfer Ratio in Head and Neck Lymphadenopathy : Comparison between Malignant and Benign Lymph Nodes¹

Sung Bum Cho, M.D., Nam Joon Lee, M.D., Myung Gyu Kim, M.D.,
Sang Il Suh, M.D., Jong Ouck Choi, M.D.²

¹Department of Diagnostic Radiology, College of Medicine, Korea University

²Department of Otolaryngology Head & Neck Surgery, College of Medicine, Korea University

Purpose: The purpose of this study was to determine whether the magnetization transfer ratio(MTR) differs between malignant and benign cervical lymphadenopathy.

Materials and Methods: Magnetization transfer ratios were obtained from 104 lymph nodes of 43 patients. Fifty-five nodes were malignant and 49 were benign. Biopsy or cervical lymph node dissection was performed in 83 nodes, while the remaining 21 were diagnosed clinically or by follow-up imaging studies. Among the 55 malignant nodes, squamous cell carcinomas accounted for 29 cases, lymphomas for 15, undifferentiated carcinomas for four, acute myelogenous leukemia for four, and melanomas for three. The 49 benign nodes comprised 21 cases of reactive hyperplasia, 12 of Kikuchi's disease, nine of acute lymphadenitis, and seven of tuberculous lymphadenitis. All scans were performed using a 1.5T Magnetom Vision(Siemens, Erlangen, Germany) with phased-array or Helmholtz-type neck coil. Scanning was performed with and without magnetization transfer pulse(MT pulse : 11.2 T, 250 Hz band-width, off-set 2.0 KHz) using FLASH 2D sequencing. The region of interest(ROI) for signal intensity(SI) measurements was sampled at the same nodes by keeping the position, shape and size of the ROI constant for the scans before and after the MT pulse was applied. SI measurements were repeated more than three times in each node and the mean value was used to calculate MTR. In this study, however, corrected MTRs(CoMTRs) were used for correction of the effect of background noise produced by magnetic field inhomogeneity.

Results: Mean CoMTRs of malignant and benign nodes were 0.33(SD: \pm 0.04) and 0.28(SD: \pm 0.05), respectively. This difference was statistically significant. At CoMTR 0.31, the sensitivity and specificity of malignant nodes were 83% and 75%, respectively.

Conclusion: A CoMTR of above 0.31 suggests malignant lymphadenopathy. CoMTR is one of the MR criteria which can serve to differentiate between malignant and benign lymphadenopathy.

Index words : Magnetic resonance(MR), tissue characterization
Magnetic resonance(MR), magnetization transfer contrast
Head and neck neoplasms, MR
Lymphatic system, MR

Address reprint requests to : Nam Joon Lee M.D. Department of Diagnostic radiology, College of Medicine, Korea University
#126-1 Anam-dong 5 ka, Sungbuk-gu, Seoul 136-705, Korea.
Tel. 82-2-920-5657 Fax. 82-2-929-3796